Eur. Phys. J. A **7**, 65–77 (2000)

THE EUROPEAN PHYSICAL JOURNAL A

EDP Sciences
© Società Italiana di Fisica
Springer-Verlag 2000

Prompt ternary break-up in ^{32}S+^{59}Co and ^{32}S+^{63}Cu reactions at 5.6 A·MeV

L. Vannucci[1], P. Boccaccio[1], A. Bologna[1], R.A. Ricci[1,2], G. Vannini[3,4], R. Donà[3,4], I. Massa[3,4], J.P. Coffin[5], P. Fintz[5], G. Guillaume[5], F. Jundt[5], F. Rami[5], P. Wagner[5]

[1] Istituto Nazionale di Fisica Nucleare, Laboratori Nazionali di Legnaro, 35020 Legnaro, Italy
[2] Dipartimento di Fisica dell'Universita'di Padova, 35100 Padova, Italy
[3] Dipartimento di Fisica dell'Universita' di Bologna, 40100 Bologna, Italy
[4] Istituto Nazionale di Fisica Nucleare, Sezione di Bologna, 40100 Bologna, Italy
[5] Centre de Recherches Nucleaires, Universite' Louis Pasteur, Strasbourg, France

Received: 3 July 1998 / Revised version: 15 October 1999
Communicated by C. Signorini

Abstract. Final states indicating the presence in the reaction of three-body fragmentation processes has been observed in ^{32}S+^{59}Co and ^{32}S+^{63}Cu dissipative collisions at 5.6 A·MeV. Besides the already observed sequential binary process, data analysis reveals the presence of prompt ternary break-up of the composite system. Indications on the system configuration at the scission have been deduced by analyzing the event shape in the momentum phase space. The decay appears to occur in a collinear configuration, one of the produced fragments originating from the neck which connects the other two. In spite of the large energy dissipation, structure effects in the charge partition seem to affect part of events.

PACS. 25.70.-z Low and intermediate energy heavy-ion reactions – 25.70.Lm Strongly damped collisions – 25.70.Pq Multifragment emission and correlations

1 Introduction

Heavy-ion reactions, producing three or more massive bodies in the final state, have been observed in a wide range of bombarding energies.

In particular, at energies above 20 A·MeV, the composite system has been observed to fragment into many pieces that can be produced by one or more sources [1-6]. Final states with fragments produced by a single source are often observed in central collisions and are due to the prompt break-up of the system. In comparison, the majority of the final states produced in peripheral collisions show the presence of several sources (frequently two) which indicates the formation and decay of excited primary fragments. In this case the reaction proceeds through several stages and sometimes for relatively long periods of time.

At energies above 20 A·MeV the prompt disassembly of the system is often associated with phenomena of compression and expansion of the nuclear matter. In the expansion phase the nuclear fluid crosses a domain of negative pressure so that the system breaks up into droplets of denser liquid embedded in lower density vapour.

At lower energies ($<$ 20 A·MeV) the fast fragmentation of the system is rarely observed because central collisions preferentially induce fusion processes (complete or incomplete). In fact, it seems established that the volume instabilities (spinodal) associated with changes of the nuclear matter density cannot take place at the lowest bombarding energies, on the contrary surface instabilities can appear. In this case the intermediate complex formed in the reaction can quickly break up into many pieces to escape from geometrical configurations [5-12] characterized by a high surface energy.

Highly deformed configurations, however, are usually produced by non-central collisions, i.e. in a region of impact parameters dominated by binary processes (fusion-fission or deep-inelastic). For this reason, at 10÷15 A·MeV final states with fragment multiplicity higher than two are mostly produced by sequential binary decays of the system.

This happens [13-20] in particular in the heavy-mass region ($A >$ 200 u) where the fission barrier is small in consequence of the strong Coulomb repulsion.

Usually, for heavy systems, the processes producing three or more massive bodies in the final state are of statistical character. In the light-mass region, however, the phenomenology often shows structure effects that, in some cases [21-23], indicate the formation of intermediate resonant states.

In the medium-mass region the fragmentation of the system into three or more heavy pieces does not seem favoured either by low fission barriers or by cluster structure of the colliding nuclei. For example, no three-body

final states have been seen in recent studies of the ^{35}Cl+^{24}Mg [24] and ^{35}Cl+^{12}C [25] reactions. However, for not much heavier systems ($A\simeq$100 u), some evidence exists [26-40] for the presence of both sequential binary decay and fast break-up in some reactions which produce three-body final states.

Therefore, the search for three-body reactions in the medium-mass region at low bombarding energy, is particularly promising for revealing different processes (fast or slow, statistical or unstatistical) and for studying their coexistence and competition in correlation with several observables.

This paper presents the study of final states produced by ^{32}S+^{59}Co and ^{32}S+^{63}Cu dissipative collisions at $E\simeq$5.6 A·MeV that indicate the presence of three-body processes in the reaction. Data analysis shows that different (dynamical or structural) effects can contribute to the fragmentation of the system.

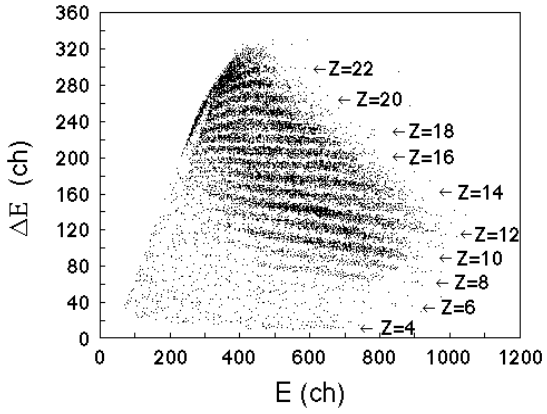

Fig. 1. ΔE-E plot (in channels) for events produced in the ^{32}S+^{63}Cu reaction

2 Experimental

The measurement was performed at the XTU tandem accelerator of the Laboratori Nazionali di Legnaro, bombarding, ^{59}Co and ^{63}Cu self supporting targets of 150 μg/cm^2 areal density with a 180 MeV ^{32}S beam.

Two fragments were detected in coincidence by two ionization chambers (IC) filled with Ar-CH_4 (90%-10%) mixture at 150 mbar pressure. Both chambers had 30° of angular acceptance (corresponding to $\simeq$65° in the c.m.) and were backed by silicon surface barrier detectors (SBD) to measure, with steps of 7.5°, the residual energy of the detected particles. Each SBD had area of 50 mm^2, was placed at 120 mm from the target and subtended a solid angle of 3.5 msr. In this way twelve different angular correlations were possible between the silicon detectors placed at θ_1 =31°, 38.5°, 46° and the others placed at θ_2 =−35°, −42.5°, −50°, −57.5° on the opposite side of the beam. In the following of the article we will assign index "1" to particles outgoing at positive angles and index "2" to particles detected at negative angles.

We measured, event-by-event, the emission angle, the energy loss inside the gas detector and the residual kinetic energy for pairs of fragments detected in coincidence. The hardware trigger logic enabled the registration of coincidence events between any pair of SBDs (not backing the same ionization chamber) within a 100 ns time window.

The particle atomic number (Z) was evaluated by using the modified power-law formula of [41], the fragment mass was deduced from the minimum in the β-stability valley corresponding to the obtained Z-value.

The calibration procedure was performed by using elastic scattering data acquired with and without gas inside the ionization chambers. By using this method it is possible to achieve a quite precise calibration of the ICs because the energy loss inside the gas can be measured, for several combinations of ions and kinetic energies, with small error ($\simeq$1%).

The obtained experimental resolution was $\simeq$1% in energy and better than one charge unit up to $Z\simeq$22 in atomic number (seen Fig. 1).

3 Results

3.1 Event selection

Three groups of events (C, B, T) are distinguishable in the scatter plot (Fig. 2) of the total measured energy (E_1+E_2) versus the total measured atomic number ($Z_1 + Z_2$).

The few events of group C are due to the reaction of the beam with target contaminants. The particle backscattering analysis of the target composition showed that only ^{12}C (5%) and ^{16}O (4%) were present in the target in not negligible quantity. Figure 2 clearly shows that the choice of relatively large observation angles was very effective in rejecting most of the two-body events originating in reactions of the beam with the Carbon or the Oxygen. We checked this bombarding a ^{12}C and a Ta_2O_5 target with a ^{32}S beam. In this test we did not find a significant contribution of events out of zones filled by the group C in the scatter plot $E_1 + E_2$ *vs.* $Z_1 + Z_2$. This result also indicates that the contribution of spurious correlations to the spectra is negligible. Therefore, the events of groups B and T can be considered as due to beam reaction with ^{59}Co and ^{63}Cu targets only.

We selected the T events in the plane $E_1 + E_2$ *vs.* $Z_1 + Z_2$. The contribution of the B events to the region of the T events was calculated by fitting the two distributions by gaussians and calculating the integral of the B-tail for $Z_1 + Z_2$ <35. We estimated that the contamination of B events in the region of T group is about 5%.

Although of different magnitude, both the groups of events (B and T) are characterized by charge deficit (ΔZ) with respect to the compound nucleus atomic number.

For B group of events we observe $\Delta Z\simeq$5 charge units (Fig. 3). This signature suggests that the B events are due to binary processes coupled to light-particle emission.

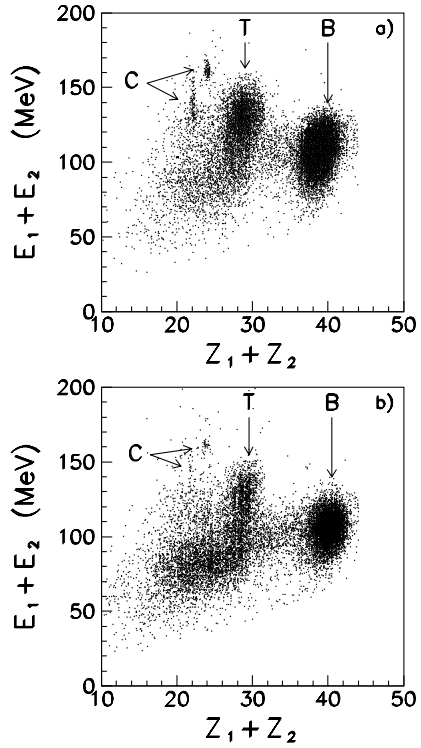

Fig. 2. Total measured kinetic energy *vs.* the total measured atomic number for pairs of detected fragments: **a** ^{32}S+^{59}Co and **b** ^{32}S+^{63}Cu reactions

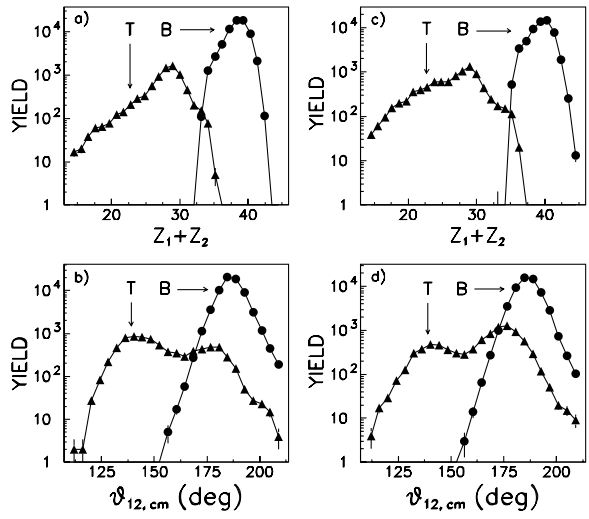

Fig. 3. Distribution of the total measured atomic number (top) and of the center of mass relative angle (bottom) for pairs of detected fragments: **a** − **b** ^{32}S+^{59}Co and **c** − **d** ^{32}S+^{63}Cu reactions

This hypothesis is also supported by the evidence that the two detected fragments Z_1 and Z_2 have a back-to-back motion (Fig. 3). Indeed, the distribution of their relative angle in the c.m. ($\theta_{12,cm}$) is rather narrow ($\pm 6°$), peaked at $\simeq$180° and practically constant for all the Z partitions.

In comparison, for the T set of events, the $\theta_{12,cm}$ distribution is broad and the charge deficit varies from 9 to 31 charge units (roughly corresponding to 18÷62 missing nucleons).

To our knowledge, no evidence is reported in literature of processes, induced by low-energy collisions, which produce so relevant an emission of light particles. So at least a third massive body should be present, although undetected, in the final state and the T group of events should be produced by ternary processes.

We assumed (in the kinematical calculation) that the third fragment corresponds to the center of mass of the undetected nuclear matter. This assumption seems realistic because the emission of some nucleons from the system does not significantly influence the kinematics. This can be seen for the binary events (group B) where the relative angle of the two detected fragments remains close to 180° in spite of the missing nucleons.

It could be argued, however, that in consequence of the light mass of the fragments, the kinematics of the T events could be more perturbed than in the case of the binary events. Moreover, as we neglect the light particle emission, the primary mass of the detected fragments could be underestimated and the primary mass of the undetected body could be overestimated. For this reason, we will show in the following sections that increasing the mass of the detected fragment by 20% and decreasing the mass of the third fragment by the same percentage, the value of the kinematical quantities does not vary enough as to change qualitative conclusions.

3.2 Two classes of three-body events

The observed three-body final states (T events) have different characteristics. In fact, in the contour plot (Fig. 4) of the total measured atomic number versus the relative angle in the c.m. ($\theta_{12,cm}$) of the two detected fragments, two groups (T_1 and T_2) are clearly distinguishable besides the group of the binary events B.

The mutual contamination of the T_1 and T_2 groups can be estimated by fitting the two distributions with gaussians and calculating the integral of each of them in the region of $\theta_{12,cm}$, where the other one is localized. By this procedure we estimated that the event contribution of each T_i group to the other one is lower than 2%.

The first group of events (T_1), peaked at $\theta_{12,cm} \simeq 140°$, has been previously studied [31-38] and characterized as due to a *sequential binary mechanism*. In this process a large part of the target is transferred to the projectile (first stage of the reaction) to form an intermediate excited complex which decays into two secondary fragments (second stage). The two steps of the reaction are uncoupled so that the outgoing direction of the two secondary fragments is randomly oriented with respect to the outgoing direction of the primary fragment that does not decay.

In comparison, in the second group, events (T_2), the two detected fragments have a back-to-back relative motion ($\theta_{12,cm} \simeq 180°$).

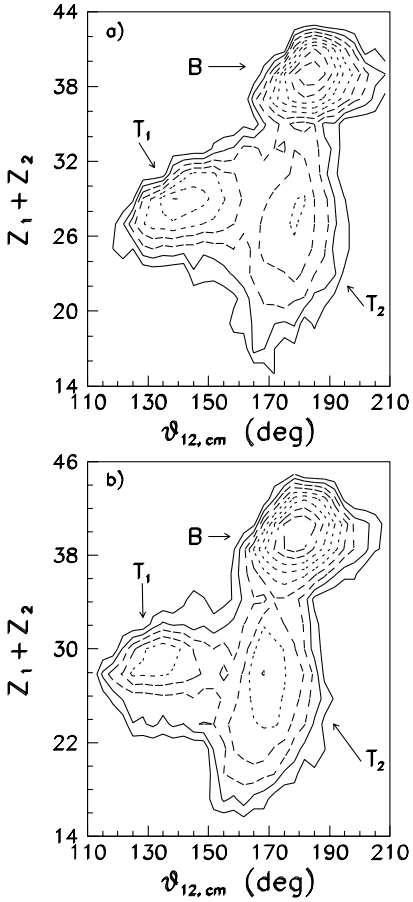

Fig. 4. Total measured atomic number versus the relative angle in the c.m. of the two detected fragments: **a** ^{32}S+^{59}Co and **b** ^{32}S+^{63}Cu reactions. The density of events defined by the contour lines is in logarithmic scale

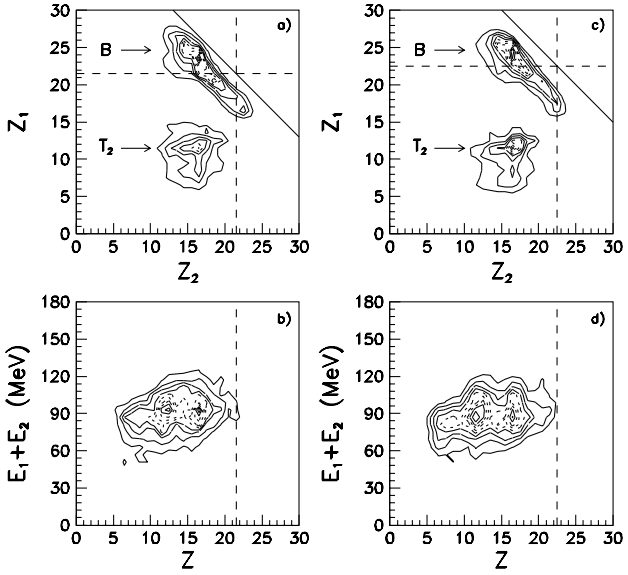

Fig. 5. **a**, **c** atomic number of one detected fragment versus atomic number of the other one for binary events (B) and events of the T_2 group, solid line represents the atomic number (Z_{tot}) of the composite system, dashed lines represent $Z_{tot}/2$. **b**, **d** E_1+E_2 *vs.* the fragment atomic number, the events have been histogrammed twice, once for each detected fragment. **a** − **b** ^{32}S+^{59}Co and **c** − **d** ^{32}S+^{63}Cu reactions

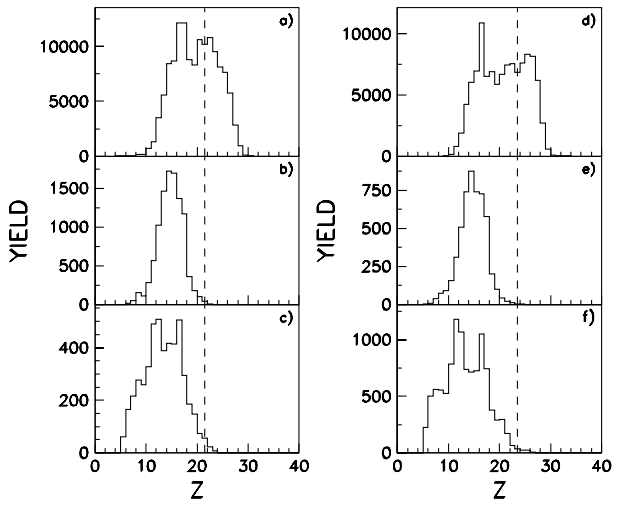

Fig. 6. **a**, **d** charge distribution from binary decays (B events in Fig. 4). **b**, **e** charge distribution from sequential binary decays (T_1 events in Fig. 4). **c**, **f** charge distribution from three-body collinear decays (T_2 events in Fig. 4). In the pictures the events have been histogrammed twice, once for each detected fragment. **a** − **c** ^{32}S+^{59}Co and **d** − **f** ^{32}S+^{63}Cu reactions

This could suggest that they are due to binary processes coupled to a large evaporation. However, it is very difficult to explain how, in reactions at 5.6 A·MeV, the light particle emission can produce a missing charge as large as the one observed.

Moreover, the binary (B) and the T_2 events have different characteristics. The binary events show, in the plot of Z_1 *vs.* Z_2, a clear charge correlation (due to their common source) that is not observed for the T_2 events (see Fig. 5).

Figure 5 shows that the T_2 events are produced in a dissipative process with charge distributions of the detected fragments clearly asymmetric (see Fig. 6).

As the events are distributed around the atomic number of the projectile, could be argued that they are produced by a deep-inelastic process. However, the large missing charge that we measured indicates that such a hypothetical deep-inelastic process should be associated to the emission of 18÷62 nucleons, via light particles, that never was observed at low bombarding energy in composite systems with mass A≃100. Alternatively it should be supposed one of the detected fragments is produced in the second step of a sequential binary process in which the target-like primary fragment breaks up after the first deep-inelastic phase. In this case, however, it is very difficult to explain the alignment of the linear momenta of the three fragments present in the final state.

The observed asymmetric cherge distributions could be compatible also with fission processes induced in medium-heavy systems, i.e. with fissility close-to or higher than the Businaro-Gallone point (x_{BG}= 0.396).

This is the case of the studied systems, ^{32}S+^{59}Co and ^{32}S+^{63}Cu, which have fissility 0.40 and 0.42, respectively. The asymmetric fission produces charge spectra with two peaks, one at atomic number lower than $Z_{tot}/2$ (where Z_{tot} is the atomic number of the composite system), the other one at higher values. The binary events (B group) present this kind of distribution (Fig. 6a,d) and the process which produces them has already been interpreted in detailed studies of the binary channel [42-45].

The charge distribution of the T_1 events (Fig. 6b,e) shows that the two detected fragments are produced by the symmetric splitting of a primary fragment with $Z\simeq 28\div 29$ generated in the first step of a sequential binary process [37,38]. In comparison, the atomic number distribution of the T_2 events shows (Fig. 6c,f) two peaks both at values lower than $Z_{tot}/2$ that, however, cannot be interpreted in the framework of the asymmetric fission.

So, although the c.m. relative angle of the two detected fragments is $\simeq 180°$, some signatures of the T_2 events are not compatible with the phenomenology of binary processes induced by low-energy collisions.

On the contrary, the observed large missing charge indicates the system breaks up into more than two heavy fragments. In this case the linear momentum of the undetected mass must be aligned (in the c.m.) with the linear momentum of the two detected fragments in consequence of their relative back-to-back motion. A similar decay mode was observed in reactions induced in heavier systems by collisions at energies >10 A·MeV [13,14].

4 Three-body events analysis

4.1 Linear momentum tensor

To evaluate quantitatively the degrees of alignment of the linear momenta we calculated, in the c.m., the linear momentum tensor of rank two [46-48]

$$p_{\alpha\beta} = \sum_{i=1}^{N} p_{i\alpha} p_{i\beta} \qquad (1)$$

where $p_{i\alpha}$ and $p_{i\beta}$ are the components in the c.m. of the linear momentum relative to the i-th particle. This tensor represents the linear momentum ellipsoid in the phase space and is determined by the linear momentum of all the N particles present in the final state.

Due to the limited acceptance of the apparatus we were able to detect only two fragments in coincidence, observing that, for part of events, the charge deficit was remarkable (from 9 to 31 charge units). As previously stressed, at low bombarding energy, a relevant missing-charge cannot be explained solely by light particle emission. Consequently, at least one non-detected fragment should be produced in the reaction. On the other hand, the low value of the collision energy does not allow the system to reach highly excited states, so that the break-up into more than three heavy fragments does not seem favoured. Therefore, we assumed that the observed T events were produced in three-body fragmentation processes.

From the analysis of the binary events (B group in Fig. 2) we deduced that the emission of some nucleons does not significantly influence the kinematics. Thus, we estimated the linear momentum of the third fragment from the linear momentum conservation, neglecting the probable presence of some light particles in the final state. Accordingly, we used a form of the linear momentum tensor suitable for three-body events [30] for the calculation:

$$p_{\alpha\beta} = \begin{pmatrix} \sum_{i=1}^{3} p_{ix}^2 & \sum_{i=1}^{3} p_{ix}p_{iy} & 0 \\ \sum_{i=1}^{3} p_{ix}p_{iy} & \sum_{i=1}^{3} p_{iy}^2 & 0 \\ 0 & 0 & 0 \end{pmatrix} \qquad (2)$$

Diagonalising this matrix we obtained its three eigenvalues $\lambda_1 > \lambda_2 > \lambda_3$ where $\lambda_3 = 0$ because of the coplanarity of the linear momenta in three-body kinematics. Therefore, the collinearity of the three fragments at the scission is characterized by the relationship:

$$\lambda = (\lambda_1 - \lambda_2)/\sqrt{\lambda_1 + \lambda_2} = 1. \qquad (3)$$

Figure 7a,b shows that λ is widely distributed for the events coming from the sequential process (T_1),whereas for the other three-body final states (T_2), it is strongly peaked at the unit indicating the alignment of the three fragments at the scission.

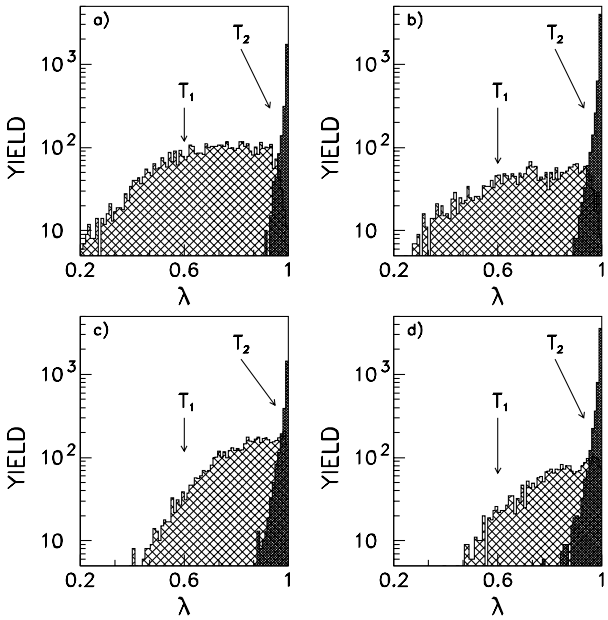

Fig. 7. Top pictures: distribution of the λ parameter for events from sequential (T_1) and collinear (T_2) fragmentation, $\lambda = 0$ indicates the exact isotropy and $\lambda = 1$ indicates the exact collinearity in the fragment emission. **c**, **d** same that **a**, **b** pictures considering a possible light particle emission of 20% of the system mass. **a**, **c** ^{32}S+^{59}Co and **b**, **d** ^{32}S+^{63}Cu reactions

In the calculation of the kinematical quantities we neglected the possible production of light particles. To estimate the effect of this process on the fragment alignment at the scission, we calculated the λ parameter from the hypothesis that 20% of the system's mass is emitted via light particles. The results show that, in particular for the T_2 events, such a process does not significantly influence the break-up configuration (compare Figs. 7a,b with Figs. 7c,d).

4.2 Three-body frequency

We estimated the acceptance of the apparatus for ternary fragmentations simulating three simple kinematical situations:

1. binary fragmentation (for B events),
2. ternary fragmentation with one body at rest in the laboratory system (for T_1 events),
3. ternary collinear fragmentation (for T_2 events).

Due to the appropriate choice of the detection angle, the efficiency of the apparatus, for ternary events, is roughly equal to the efficiency for binary events in the case of the ^{32}S+^{59}Co reaction and a little lower ($\simeq$78%) for ^{32}S+^{63}Cu. From this estimation and the measured frequencies of the ternary events we deduced the branching ratios of the three body events with respect to the binary ones. In the region of the phase space covered by the experimental set-up, the observed three body final states are produced with probability which varies from 10% to 20% of the binary events, depending on the reaction.

These results were obtained assuming (for simplicity) that the undetected fragment, in the case of the T_1 events, is produced at rest in the laboratory system and that, in the case of the T_2 events, it has (in the c.m.) linear momentum exactly aligned with the momentum of the two detected fragments.

For an estimation of the absolute cross section of the three-body events can be used the experimental cross sections [42-45] of binary processes induced in ^{32}S+^{59}Co and ^{32}S+^{63}Cu systems by collisions at bombarding energy close the one used in the present study.

4.3 Break-up configuration

In the case of the T_2 events, the alignment of the c.m. linear momenta indicates the system fragments in collinear configuration and resembles, at break-up, a chain of three aligned pieces of nuclear matter.

In this situation the piece placed in the middle of the chain should have, in the c.m., a velocity lower than the fragments placed at the ends because they exert opposite repulsion on it.

Figure 8 shows that the velocity of the undetected fragment (Z_3) is compatible with the previoulsly described break-up configuration because, in most of the cases, the velocity of the two detected fragments is higher than v_{3cm}.

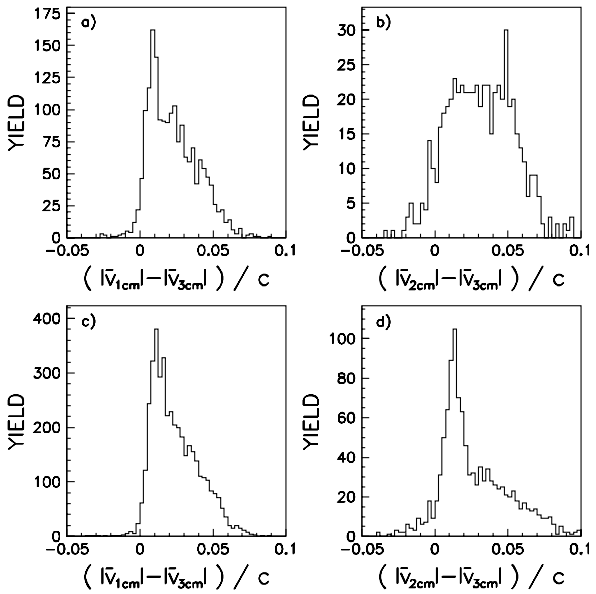

Fig. 8. Difference between the c.m. velocity of detected fragments (Z_1 and Z_2) and the velocity of the undetected one (Z_3). **a** − **b** ^{32}S+^{59}Co and **c** − **d** ^{32}S+^{63}Cu reactions

The velocities of the two detected fragments were calculated from the measured kinetic energies by using as fragment mass the minimum in the β-stability valley corresponding to the measured atomic number. In the case of the third body, its velocity was deduced from its linear momentum instead, which was calculated using linear momentum conservation.

If the third fragment is really placed in the middle of the break-up configuration the relative energy (E_{12}) of the other two fragments is expected to increase with Z_3 because of the increasing of the Coulomb repulsion exerted by it. This phenomenon is evident for both the studied system and can be seen in Fig. 9, where the error bars represent the FWHM of the distributions whereas the error on the determination of their mean value is smaller than the symbol size. In Fig. 9 in order to avoid dependence on the $Z_1 \div Z_2$ partition, E_{12} was normalized to the Coulomb potential V_C.

From Fig. 9 it is also deducible that, in the collinear fragmentation process (T_2 events), the three produced fragments are interacting strongly at the scission. As expected, this does not happen in the sequential binary process (T_1 events) where the relative energy of the two secondary fragments (the two detected) is not influenced by the size of Z_3, because the source that gives origin to them decays far from the third body.

Concluding, the evident mutual interaction of the three fragments in the final state and the alignment of the fragment linear momentum at the scission strongly indicate that the T_2 events are produced in a *fast break-up process*.

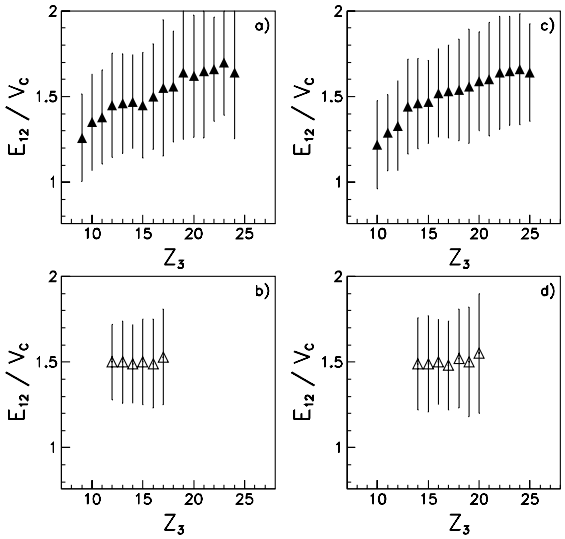

Fig. 9. Relative energy of the two detected fragments, normalized to the Coulomb potential, as a function of the atomic number of the third fragment for collinear fragmentations (top) and sequential binary decay (bottom). Error bars represent the FWHM of the distributions whereas the error on the mean value is smaller than the symbol size. **a**−**b** ^{32}S+^{59}Co and **c**−**d** ^{32}S+^{63}Cu reactions

4.4 Reaction centrality dependence

In heavy-ion reactions, at low bombarding energy, the fast processes are usually related to peripheral collisions. In order to evaluate the centrality of the collision we calculated the parameter $Y_3 =< v_{rel} > -(v_{rel})_{min}$ [49] which estimates the dispersion of the relative velocities of the fragments. Indeed, low values of Y_3 are correlated with small impact parameters, whereas high Y_3-values indicate peripheral collisions.

Figure 10 shows that the Y_3 distributions for the T_1 and the T_2 events are partially overlapping, indicating that the two processes might be in competition. The events from sequential binary decay (T_1 group) appear correlated with small impact parameters, whereas the collinear fragmentations (T_2 group) seem originated in more peripheral collisions.

This suggests that different elongations can characterize the configuration of the composite system at the scission and induce different evolutions. In binary fission processes, for example, the stretching of the system can lead to configurations similar to two spheres connected by a cylindrical neck. At the system scission the neck breaks up in a single point, its two residual pieces are reabsorbed by the fission fragments and then only two massive bodies are produced in the final state. In very elongated configurations (mostly expected for heavy systems) the break-up of the neck may occur in several points, so that fission fragments can also be produced from the region of the neck, and the linear momenta are aligned in the final state.

This scenario is compatible with the phenomenology of the ternary collinear fragmentations observed in our measurement.

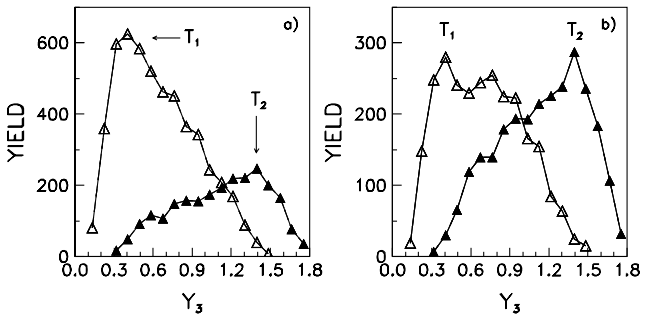

Fig. 10. Y_3 distribution for sequential (T_1) and collinear (T_2) three-body fragmentations: **a** ^{32}S+^{59}Co and **b** ^{32}S+^{63}Cu reactions

Another remarkable point is that the size of the third fragment (Z_3) which is produced in the central region of the system, increases with the impact parameter (Fig. 11), as is expected for increasingly elongated configurations in which the quantity of nuclear matter present in the neck becomes larger and larger.

This effect is completely absent in the events originating in the sequential binary process where the third fragment (Z_3) is produced in the first binary splitting of the system [38]. Therefore, no correlation exists between the impact parameter and the size of the third fragment which remains practically constant with Y_3. On the contrary, such a correlation, which is evident for the collinear fragmentations (T_2 events), indicates that the third fragment is produced from the central region of the system.

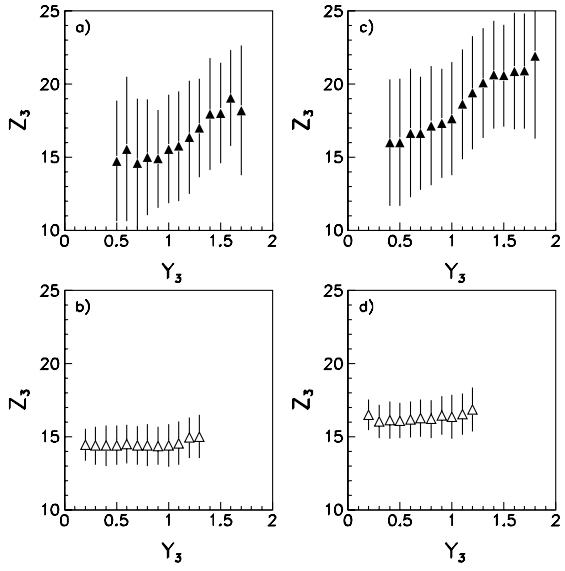

Fig. 11. Size of Z_3 as a function of Y_3 for collinear fragmentations (top) and sequential binary decay (bottom). Error bars represent the FWHM of the distributions whereas the error on the mean value is smaller than the symbol size. **a**−**b** ^{32}S+^{59}Co and **c** − **d** ^{32}S+^{63}Cu reactions

4.5 Fragment kinetic energy

From the position of the three fragments in the break-up configuration it is also possible to guess the system's shape at the scission. In fact this shape affects the fragment-fragment potential and the rotational energy (through the moment of inertia) which both influence the asymptotic kinetic energy of the outgoing fragments.

We calculated the kinetic energy of the three fragments produced in the reaction for some simple scission-shapes and found that the best agreement with the data is obtained assuming a break-up configuration formed by two spheres (the two detected fragments) connected by a cylindrical neck (the missing one). In our hypothesis, the system evolves from the initial configuration, formed by two touching spheres (projectile and target), towards the final configuration without a significant stretching. An usual parameterization of the radius ($R = 1.2{\cdot}A^{1/3}$ fm) was assumed in the calculation. Although the system is not stretched, it has an elongated shape because the ratio between the longer symmetry axis and the two shorter ones is about three. We assumed that the energy of the system at the scission is the sum of the nuclear (V_N) [50], the Coulomb (V_C) potential and the rotational energy (E_R). This last term is calculated from the difference between the sum of the kinetic energy of the three fragments in the final state (TKE) and the sum of the nuclear and the Coulomb potential ($E_R = TKE - V_N - V_C$). In this way the calculated total kinetic energy matches exactly with the experimental value, however, the calculated kinetic energy of each individual fragment depends on the shape of the system at the scission.

Figure 12 shows a fair agreement of the calculation with the measured kinetic energies. This indicates that the geometrical shape we assumed described the system configuration at the scission is quite realistic and, consequently, the moment of inertia of the system does not substantially differ from the calculated value.

In this condition it is possible to estimate, from the rotational energy, the total angular momentum (l_{tot}).

Due to the angular momentum conservation, this quantity matches with the entrance channel angular momentum and provides information about the impact parameter. It must be noted that for the calculation of l_{tot} and Y_3 a different experimental information is used; in the first case the fragment velocity (i.e. the kinetic energy), in the second case the dispersion of the (relative) velocities. However, both the quantities (l_{tot} and Y_3) represent the same physical observable: the centrality of the collision, and should be correlated. This allows us to check both the consistency of the procedure adopted to determine the fragment kinetic energy and the reliability of the information on the centrality of the collision given by Y_3.

Figure 13 clearly shows the presence of this physical correlation. On the other hand the flat behaviour of l_{tot} *vs.* Y_3 (Fig. 13b) for Y_3<1 indicates that these two observables are not necessarily correlated by a mathematical relation. The small contamination (≃6%) of the T_2 events, due to spurious correlations coming from the B and the T_1 groups, does not produce visible changing in the pictures.

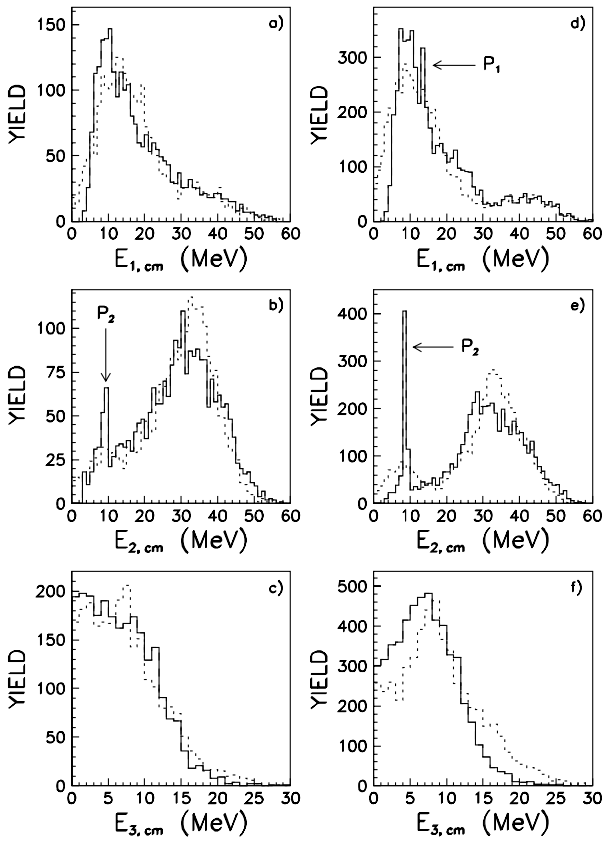

Fig. 12. Kinetic energy in the c.m. of the three fragments produced in the collinear fragmentations. Solid lines correspond to experimental values and dot lines correspond to calculated values. P_1 and P_2 indicate classes of events which show a strong fragment-fragment correlation (see text). **a** − **c** ^{32}S+^{59}Co and **d** − **f** ^{32}S+^{63}Cu reactions

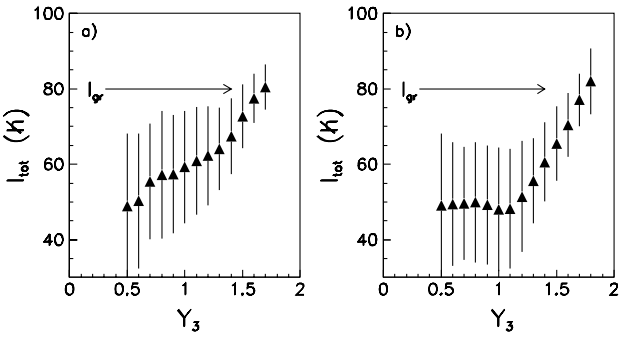

Fig. 13. Entrance channel angular momentum (l_{gr} grazing angular momentum) as a function of the Y_3 parameter. Error bars represent the FWHM of the distributions whereas the error on the mean value is smaller than the symbol size. **a** ^{32}S+^{59}Co and **b** ^{32}S+^{63}Cu reactions

This was checked by adding B and T_1 events, randomly distributed, to the T_2 group in quantities of 5% and 1% of the T_2 counts, respectively.

There also seems to exist (see in particular Fig. 13b) a minimum value ($l_{tot}\simeq 40\ \hbar$)of the entrance channel angular momentum for which the ternary collinear fragmentation of the system is possible. This minimum value, however, could not have a physical meaning but could merely indicate a loss of sensitivity in the correlation between Y_3 and l_{tot}. Anyway, the presence in the reaction of many partial waves beyond this limits ($\simeq 40\ \hbar$) shows that the process is mostly due to peripheral collisions.

These l-values, however, in some model calculations [51] do not seem sufficient to induce the system break-up via ternary fission. Indeed, in the $A\simeq 100$ u mass region the fission barrier is quite high both for binary and ternary fragmentation. Moreover, the effect of the nucleus heating is not considerable because for temperatures of $2\div 3$ MeV, as in our case, the decreasing of the fission barrier is smaller than ten MeV. Instead, a remarkable effect should have the shape assumed by the system at the scission. In fact the angular momentum at which the ternary fission barrier is expected to vanish is reduced by a factor of two from symmetric to asymmetric fragmentations [51]. Therefore, ternary fission processes might produce the observed collinear fragmentations in the ^{32}S+^{59}Co and ^{32}S+^{63}Cu reactions provided that the system reaches an appropriate saddle-point shape.

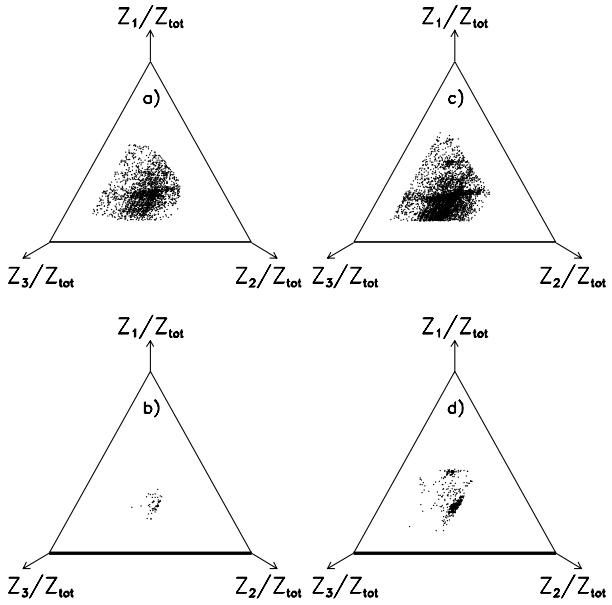

Fig. 14. Dalitz-plots of the fragment atomic number for the full set of T_2 events (top) and for the subsets P_1 and P_2 (bottom). **a** − **b** ^{32}S+^{59}Co and **c** − **d** ^{32}S+^{63}Cu reactions

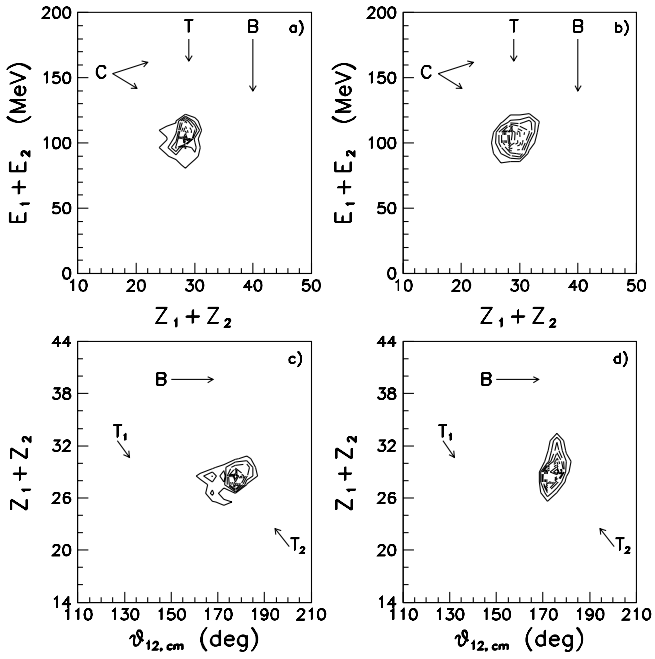

Fig. 15. P_1 and P_2 events. Top pictures: total measured kinetic energy *vs.* total measured atomic number. Bottom pitsures: total measured atomic number *vs.* relative angle in the c.m.. **a** ^{32}S+^{59}Co and **b** ^{32}S+^{63}Cu reactions

4.6 Fragment-fragment correlation

The analysis of the kinetic energies also shows that, in some cases, the results of our calculations disagree with the data. In particular in the kinetic energy spectra (see Fig. 12) some narrow peaks (P_1 and P_2) are present that the calculations completely fail to reproduce. This does not depend on different system shapes at the scission because the phenomenology indicates that the break-up occurs always in collinear configuration.

The effect never seems due to kinematics cuts. In fact, the Dalitz-plots of the fragment atomic number (Fig. 14a and Fig. 14c), present regions not covered by the apparatus acceptance only in the corners Z_1/Z_{tot} and Z_2/Z_{tot}. The other evident cuts at low atomic number are due to software event selection required to have three massive fragments ($Z_i > 6$) in the final state. These cuts, however, have no influence on the P_1 and P_2 distributions that appear placed in the middle of the Dalitz-plots and not near the borders (see Fig. 14b and Fig. 14d).

Moreover, also in the scatter plots E_1+E_2 *vs.* Z_1+Z_2 (Fig. 15a,b) and Z_1+Z_2 *vs.* $\theta_{12,cm}$ (Fig. 15c,d), the P_1 and P_2 events are localized in the middle and not near the border.

So, the narrow peaks observed in the energy spectra are not due to instrumental effects and the particular phenomenology of the P_1 and P_2 events is due to the reaction mechanism.

The narrow peaks of Fig. 12 correspond, in the scatter plot of the kinetic energy of one detected fragment versus the kinetic energy of the other one, to narrow bands (see Fig. 16). Such a topology indicates correlation between the produced fragments [52] and that there exists preferential decay modes of the system.

In particular, the reaction systematically produces Silicon in the ^{32}S+^{59}Co collisions and Calcium (P_1 final states) or Sulphur (P_2 final states) in the ^{32}S+^{63}Cu collisions (see Table 1 and 2). Consequently, as the atomic

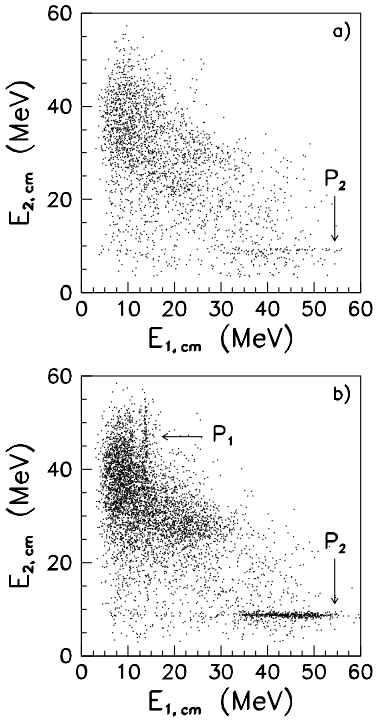

Fig. 16. Scatter plot of the kinetic energy in the c.m. of one detected fragment versus the kinetic energy of another. P_1 and P_2 indicate classes of events which show a strong fragment-fragment correlation (see text). **a** ^{32}S+^{59}Co and **b** ^{32}S+^{63}Cu reactions

Table 1. Atomic number of the three fragments produced in collinear fragmentations of the ^{32}S+^{59}Co system

	Z_1	Z_2	Z_3
	13	14	16
P_2 events	13	16	14
	12	17	14
other events	6÷23	6÷22	8÷30

Table 2. Atomic number of the three fragments produced in collinear fragmentations of the ^{32}S+^{63}Cu system

	Z_1	Z_2	Z_3
P_1 events	20	11	14
	20	12	13
	11	16	18
P_2 events	12	16	17
	13	16	16
other events	6÷26	6÷22	10÷30

number of one of the fragments is fixed, the other two fragments are strongly Z-correlated. However, not all the possible Z-partitions between these two fragments are observed, only some of those which produce at least one nucleus close to the Magnesium (Table 1 and Table 2).

Therefore, while the majority of the events has fragment atomic number distributed in a wide range, the process producing the P_1 and P_2 events selectively populates final states in which at least one fragment is an α-like nucleus indicating the possible presence of clustering phenomena in the reaction.

4.7 Energy dissipation and relaxation process

Additional information on the collinear fragmentation process can be deduced from the analysis of the energy dissipation and of the centrality of the collision.

Figure 17 shows that the reaction is very dissipative because the damped energy ($-Q$=E_{cm}-TKE) increases from 40 until 70 MeV with the increasing of the centrality of the collision. The large inelasticity (on an average $\simeq$54% of entrance channel kinetic energy) justifies the low velocity of the undetected fragment.

The process producing the P_1 and P_2 events is clearly peripheral, so that the preferential break-up of the system in fragments similar to α-like nuclei, could be favoured by the preformation of a ternary clustered configuration which does not evolve in a mono-nuclear regime.

Non-equilibrium effects have been observed in ternary collinear decays of a stretched intermediate system formed in the ^{100}Mo+^{100}Mo and the ^{120}Sn+^{120}Sn collisions at 18.7 and 18.4 A·MeV respectively [14]. In this experiment an anisotropy of the in-plane angular distributions was found particularly evident for the asymmetric mass division. This peaking implies that levels with different angular momenta contribute coherently to the decay. The observed effect was interpreted in the framework of the

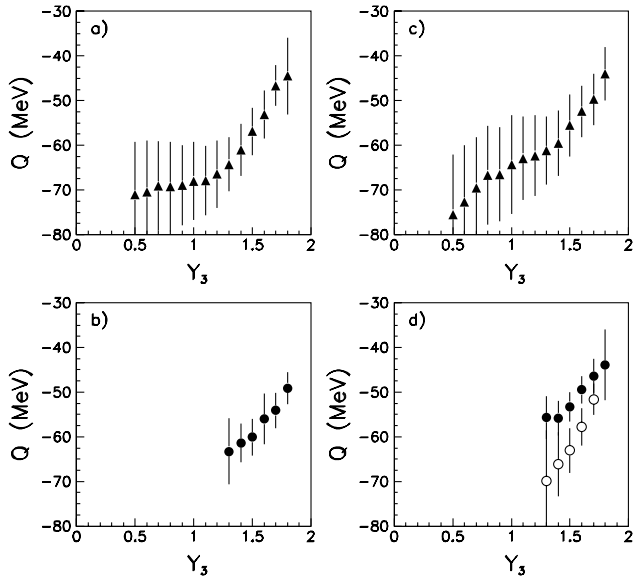

Fig. 17. Q-value versus Y_3 for the full set of T_2 events (top pictures) and the P_1 (circles) and P_2 (dots) subsets (bottom pictures). Error bars represent the FWHM of the distributions whereas the error on the mean value is smaller than the symbol size. **a** − **b** ^{32}S+^{59}Co and **c** − **d** ^{32}S+^{63}Cu reactions

model proposed by Kun in [53]. In the Kun model, the formation of the intermediate state is due to the preferential excitation of a large number of rotational levels in a dinuclear system. This process is completely different from the usual compound nucleus picture based on the assumption that levels of a very different nature are excited in the fusion process. This assumption justifies the complete absence of correlation among different angular momenta contributing to the reaction and the isotropic in-plane angular distributions. In comparison, in the Kun model, the level overlapping and their common rotational character originate from an angular-momentum coherence of pole form and focusing effects in the in-plane angular distributions like the ones observed in deep-inelastic dissipative collisions. The anisotropy of the angular distributions vanishes for a large rotation of the system and for long-living intermediate states that have enough time to equilibrate. Therefore, in the Kun model the system behaves as a rotating macroscopic quasi-molecular object characterized by a collective angular velocity ω.

These kind of non-equilibrated states were found in medium-mass systems and, in particular, in the two-body channel of the ^{19}F+^{89}Y [53], ^{28}Si+^{48}Ti [54–56], ^{58}Ni+^{58}Ni, ^{58}Ni+^{64}Ni [57] and ^{58}Ni+^{46}Ti reactions [58]. They could also be present in three-body channels.

A hint of this possibility is shown by the flow-angle distribution of the events produced in the collinear fragmentation process. The flow-angle (θ_{fw}) is given by the orientation of the largest axis of the linear momentum ellipsoid in the c.m.. Although the shape of the ellipsoid is determined by the linear momentum of all the particles in the final state, in the present case, for the reasons previously discussed, we assumed the presence of only three fragments.

As one can see in Fig. 18 the events due to the collinear fragmentation of the system practically fill all the apparatus angular acceptance (40°÷130°) with a broad distribution. In comparison, the subsets P_1 and P_2, which show structure effects in Z-partition and fragment-fragment correlation, are associated with narrow θ_{fw} peaks which indicate the formation of short-living intermediate states.

Assuming that the θ_{fw} distribution mainly reflects the interplay between the system's rotational frequency and its life-time it is possible to deduce the reaction time-scale simply from the ratio between the average rotational angle (θ_{rot}) and the average angular velocity (ω).

The average rotational angle is the sum of the grazing angle with the flow-angle. Unfortunately it is not possible to calculate unambiguously θ_{rot} without knowing if the fragment, emitted in the direction of the flow-angle, is produced by the projectile or by the target. In fact, the projectile has a forward grazing angle whereas the target has a backward grazing angle. However, for the P_2 set of events, the fragment Z_2 is emitted at angles close to θ_{fw} and its atomic number matches the projectile atomic number or differs a little bit from it (see Table 1 and 2). Therefore, for the P_2 group of events, the average rotational angle should be $\theta_{rot}=\theta_{gr}+\theta_{fw}\simeq 40°+110°=150°$ and the break-up of the system should occur before a complete rotation. For peripheral collisions like the ones that produce the P_1 and P_2 events, we estimated an average angular velocity of the system of $\omega\simeq 1.4\cdot 10^{21}$ rad/s and from it a reaction time of $\tau=\theta_{rot}/\omega<2\cdot 10^{-21}$ s.

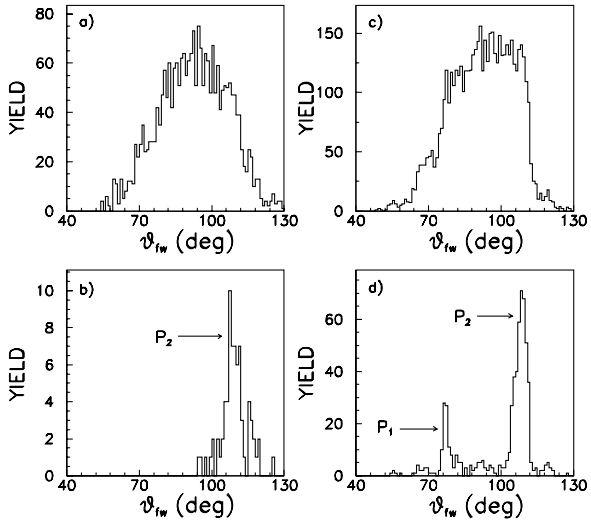

Fig. 18. Flow-angle distribution for the full set collinear fragmentation events (top) and for the subsets P_1 and P_2 (bottom). **a** − **b** ^{32}S+^{59}Co and **c** − **d** ^{32}S+^{63}Cu reactions

Usually, a so short time-scale is not considered sufficient to equilibrate all the system degrees of freedom, in particular the ones which have a long relaxation time-constant as the system shape. Consequently, the process inducing the collinear fragmentation of the system should produce intermediate states having different degrees of equilibration and, probably, could produce macroscopic quasi-molecular states like the ones described by the Kun model [53]. To check this hypothesis, however, measurements of excitation functions and evidences of non-statistical structures in the ternary collinear fragmentation channel are necessary.

5 Conclusion

Final states indicating the presence of both sequential and prompt fragmentation of the system in three massive bodies has been observed in the ^{32}S+^{59}Co and ^{32}S+^{63}Cu reactions at low bombarding energy (E_{lab}=180 MeV).

This paper, in particular, presents the study of the events produced in fast break-up processes.

Indications on the system configuration at the scission have been deduced by analyzing the event shape in the momentum phase space and the fragment kinetic energy spectra. The decay appears to occur in a collinear configuration, one of the produced fragments originating from the neck which connects the other two.

The centrality of the collision was estimated from the dispersion of the fragment's relative velocities through the Y_3 parameter. The events from collinear fragmentation ap-

pear to originate in collisions more peripheral than the events generated by sequential binary decay.

The large inelasticity of the process indicates that the reaction threshold is not much lower than 6 A·MeV.

In spite of the large energy dissipation, some of events shows structure effects, i.e. the possible presence of clustering phenomena in the reaction (at least one fragment is an α-like nucleus). In particular, the analysis in terms of the Y_3 parameter indicates that the events which show structure effects are due to the most peripheral trajectories.

References

1. D'Agostino, M., Kunde, G.J., Milazzo, P.M., Diniu, J.D., Bruno, M., Colonna, N., Fiandri, F., Gelbke, C.K., Glasmacher, T., Gramegna, F., Handzy, D.O., Hsi, W.C., Huang, M., Lisa, M.A., Lynch, W.G., Mastinu, P.F., Montoya, C.P., Moroni, A., Peaslee, G.F., Phair, L., Rui, R., Schwarz, C., Tsang, M.B., Vannini, G., Williams, C.: Phys. Rev. Lett. **75**, 4373 (1995)
2. D'Agostino, M., Mastinu, P.F., Milazzo, P.M., Bruno, M., Bowman, D.R., Buttazzo, P., Celano, L., Colonna, N., Dinius, J.D., Ferrero, A., Fiandri, M.L., Gelbke, C.K., Glasmacher, T., Gramegna, F., Handzy, D.O., Horn, D., Hsi, W.C., Huang, M., Iori, I., Kunde, G.J., Lisa, M.A., Lynch, W.G., Manduci, L., Margagliotti, G.V., Montoya, C.P., Moroni, A., Peaslee, G.F., Petruzzelli, F., Phair, L., Rui, R., Schwarz, C., Tsang, M.B., Vannini, G., Williams, C.: Phys. Lett. B**368**, 259 (1996)
3. D'Agostino, M., Botvina, A.S., Milazzo, P.M., Bruno, M., Kunde, G.J., Bowman, D.R., Buttazzo, P., Celano, L., Colonna, N., Dinius, J.D., Ferrero, A., Fiandri, M.L., Gelbke, C.K., Glasmacher, T., Gramegna, F., Handzy, D.O., Horn, D., Hsi, W.C., Huang, M., Iori, I., Lisa, M.A., Lynch, W.G., Manduci, L., Margagliotti, G.V., Mastinu, P.F., Mishustin, I.N., Montoya, C.P., Moroni, A., Peaslee, G.F., Petruzzelli, F., Phair, L., Rui, R., Schwarz, C., Tsang, M.B., Vannini, G., Williams, C.: Phys. Lett. B**371**, 175 (1996)
4. Belkacem M., Mastinu P.F., Latora V., Bonasera A., D'Agostino, M.,Dinius, J.D., Fiandri, M.L., Gramegna, F., Handzy, D.O., Hsi, W.C., Huang, M., Margagliotti, G.V., Milazzo, P.M., Montoya, C.P., Peaslee, G.F., Rui, R., Schwarz, C., Vannini, G., Williams, C.: Phys. Rev. C**54**, 2435 (1996)
5. Moretto, L.G., Wozniak, G.J.: Ann. Rev. Nucl. Part. Sci. **43**, 379 (1993)
6. Moretto, L.G., Ghetti, R., Phair, L., Tso, K., Wozniak, G.J.: Phys. Rep. **287**, 249 (1997)
7. Moretto, L.G., Tso, K., Colonna, N., Wozniak, G.J.: Phys. Rev. Lett. **69**, 1884 (1992)
8. Brosa, U., Grossmann ,S., Müller, A., Becker, E.: Nucl. Phys. A**502**, 423c (1989)
9. Brosa, U., Grossmann, S., Müller, A.: Phys. Rep. **197**, 167 (1990)
10. Borderie, B., Remaud, B., Rivet, M.F., Sebille, F.: Phys. Lett. B**302**, 15 (1993)
11. Bauer, W., Bertsch, G.F., Shulz, H.: Phys. Rev. Lett. **69**, 1888 (1992)
12. Kartavenko, V.G. Preprint JINR E4-92-463, Dubna, 1992
13. Glässel, P., Harrach, D.V., Specht, H.J., Grodzins, L.: Z. Phys. A**310**, 189 (1983)
14. Casini, G., Bizzeti, P.G., Maurenzing, P.R., Olmi, A., Stefanini, A.A., Wessels, J.P., Charity, R.J., Freifelder, R., Gobbi, A., Herrmann, N., Hildenbrand, K.D., Stelzer, H.: Phys. Rev. Lett. **71**, 2567 (1993)
15. Charity, R.J., Freifelder, R., Gobbi, A., Herrmann, N., Hildenbrand, K.D., Rami, F., Stelzer, H., Wessels, J., Casini, G., Maurenzing, P.R., Olmi, A., Stefanini, A.A., Galin, J., Guerreau, D., Jahnke, U., Adloff, J.C., Bilwes, B., Bilwes, R., Rudolf, G., Petrovici, M., Gnirs, M., Pelte, D. Report dell'Università di Firenze DFF 123/12/'90
16. Olmi, A.: Nucl. Phys. A**471**, 100c (1987)
17. Casini, G., Stefanini, A.A., Bini, M., Maurenzing, P.R., Olmi, A., Poggi, G., Charity, R.J., Freifelder, R., Gobbi, A., Hildenbrand, K.D., Tanaka, M.H., Wessels, J.P.: Phys. Rev. Lett. **24**, 3364 (1991)
18. Olmi, A., Maurenzing, P.R., Stefanini, A.A., Albinski, J., Gobbi, A., Gralla, S., Herrmann, N., Hildenbrand, D.K., Kuzminski, J., Müller, W.F.J., Petrovici, M., Stelzer, H., Toke, J.: Europhys. Lett. **4**, 1121 (1987)
19. Cârjan, N., Sierk, A.J., Nix, J.R.: Nucl. Phys. A**452**, 381 (1986)
20. Harrach, D.V., Glässel, P., Civelekoglu, Y., Männer, R., Specht, H.J.: Phys. Rev. Lett. **42**, 1728 (1979)
21. Costanzo, E., Lattuada, M., Romano, S., Vinciguerra, D., Zadro, M., Cindro, N., Freer, M., Fulton, B.R., Rae, W.D.M.: Europhys. Lett. **14**, 221 (1991)
22. Costanzo, E., Lattuada ,M., Romano, S., Vinciguerra, D., Cindro, N., Zadro, M., Freer, M., Fulton, B.R., Rae, W.D.M.: Phys. Rev. C**44**, 111 (1991)
23. Costanzo, E., Lattuada, M., Pirrone, S., Romano, S., Vinciguerra, D., Zadro, M.: Phys. Rev. C**49**, 985 (1994)
24. Nouicer, R., Beck, C., Mahboub, D., Matsuse, T., Djerroud, B., Freeman, R.M., Hachem, A., Cavallaro, Sl., De Filippo, E., Lanzanò, G., Pagano, A., Sperduto, M.L., Dayras, R., Berthoumieux, E., Legrain, R., Polacco, E.: Z. Phys. A**356**, 5 (1996)
25. Beck, C., Mahboub, D., Nouicer, R., Matsuse, T., Djerroud, B., Freeman, R.M., Haas, F., Hachem, A., Morsad, A., Youlal, M., Sanders, S.J., Dayras, R., Wieleczko, J.P., Berthoumieux, E., Legrain, Polacco, E., Cavallaro, Sl., De Filippo, E., Lanzanò, G., Pagano, A., Sperduto, M.L., R.: Phys. Rev. C**54**, 227 (1996)
26. Boger, J., Kox, S., Auger, G., Alexander, J.M., Narayanan, A., McMahan, M.A., Moses, D.J., Kaplan, M., Gilfoyle, G.P.: Phys. Rev. C**41**, R801 (1990)
27. Winkler, U., Weissman, B., Bühler, M., Gorks, A., Novotny, R., Pelte, D.: Nucl. Phys. A**425**, 573 (1984)
28. Pelte, D., Winkler, U., Pochodzalla, J., Bhler, M., Gorks, A., Weissmann, B.: Nucl. Phys. A**438**, 582 (1985)
29. Pelte, D., Winkler, U., Bühler, M., Weissmann, B., Gobbi, A., Hildenbrand, K.D., Stelzer, H.: Phys. Rev. C**34**, 1673 (1986)
30. Pelte, D., Winkler, U., Gnirs, M., Gobbi, A., Hildenbrand, K.D., Novotny, R.: Phys. Rev. C**39**, 553 (1989)
31. Vannini, G., Massa, I., Lavagnini, L., Boccaccio, P., Vannucci, L., Ricci, R.A., Iori, I., Coffin, J.P., Fintz, P., Gonin, M., Guillaume, G., Heusch, B., Jundt, F., Malki, A., Rami, F., Wagner, P.: Europhys. Lett. **7**, 311 (1988)
32. Boccaccio, P., Mwose, P.K., Vannucci, L., Bettiolo, M., Ricci, R.A., Augustyniak, W., Massa, I., Vannini, G., Cof-

fin, J.P., Fintz, P., Guillaume, G., Heusch, B., Jundt, F., Rami, F., Wagner, P.: Il Nuovo Cimento A**106**, 379 (1993)
33. Vannucci, L., Bettiolo, M., Boccaccio, P., Donà, R., Ricci, R.A., Augustyniak, W., Massa, I., Vannini, G., Coffin, J.P., Fintz, P., Guillaume, G., Heusch, B., Jundt, F., Rami, F., Wagner, P. Proceedings of the International Symposium on Time Characteristics of Nuclear Reactions, p.72, September 20-25, 1993, Moscow, Russia
34. Vannucci, L., Boccaccio, P., Ricci, R.A., Vannini, G., Donà, R., Massa, I., Coffin, J.P., Fintz, P., Guillaume, G., Jundt, F., Rami, F., Wagner, P. Proceedings of the International Symposium on Large-Scale Collective Motion of Atomic Nuclei, October 15-19, 1996, Brolo, Italy
35. Vannucci, L., Boccaccio, P., Ricci, R.A., Vannini, G., Donà, R., Massa, I., Coffin, J.P., Fintz, P., Guillaume, G., Jundt, F., Rami, F., Wagner, P. Proceedings of the International Workshop on New Ideas on Clustering in Nuclear and Atomic Physics, June 3-9, 1997, Rauischholzhausen Castle, Germany
36. Vannucci, L., Boccaccio, P., Ricci, R.A., Vannini, G., Donà, R., Massa, I., Coffin, J.P., Fintz, P., Guillaume, G., Jundt, F., Rami, F., Wagner, P. Proceedings of the 2nd Latinamerican Workshop on Nuclear Physics and Heavy Ion Reactions September 1-5, 1997, Caracas, Venezuela
37. Boccaccio, P., Bettiolo, M., Donà, R., Vannucci, L., Ricci, R.A., Vannini, G., Massa, I., Coffin, J.P., Fintz, P., Guillaume, G., Jundt, F., Rami, F., Wagner, P.: Z. Phys. A**354**, 121 (1996)
38. Boccaccio, P., Vannucci, L., Ricci, R.A., Vannini, G., Donà, R., Massa, I., Coffin, J.P., Fintz, P., Guillaume, G., Jundt, F., Rami, F., Wagner, P.: Eur. Phys. J. A**1**, 399 (1998)
39. Padalino, S.J., Putnam, M.A., Constable, J.A., De Clerck, T.G., Dennis, L.C., Zingarelli, R., Kline, R., Sartor, K.: Phys. Rev. C**41**, 594 (1990)
40. Petrascu, M., Isbasescu, A., Lazar, I., Mihai, I., Petrascu, H., Rudchik, A.T., Chernievski, V.A., Ponkratenko, O.A., Ziman, V.A.: Z. Phys. A**345**, 395 (1993)
41. Butler, G.W., Poskanzer, A.M., Ladis, D.A.: Nucl. Instr. Meth. **89**, 189 (1970)
42. Iori, I., Gentili, M., Massa, I., Vannini, G., Boccaccio, P., Reffo, F., Vannucci, L., Ricci, R.A.: Phys. Lett. B**132**, 304 (1983)
43. Gentili, M., Massa, I., Vannini, G., Boccaccio, P., Reffo, F., Vannucci, L., Ricci, R.A., Iori, I.: Lettere al Nuovo Cimento **40**, 505 (1984)
44. Agnoli, S., Massa, I., Vannini, G., Boccaccio, P., Reffo, F., Vannucci, L., Iori, I., Ricci, R.A.: Nucl. Phys. A**464**, 103 (1987)
45. Boccaccio, P., Vannucci, L., Bettiolo, M., Lavagnini, L., Vannini, G., Massa, I., Ricci, R.A., Iori, I., Guillaume, G., Coffin, J.P., Fintz, P., Rami, F.: Phys. Rev. C**38**, 2108 (1988)
46. Gyulassy, M., Frankel, K.A., Stöker, H.: Phys. Lett. B**110**, 185 (1982)
47. Cugnon, J., L'Hote, D.: Nucl. Phys. A**397**, 519 (1983)
48. Knoll, J.: Phys. Scripta T**5**, 118 (1983)
49. Bougault, R., Delaunay, F., Genoux-Lubain, A., Le Brun, C., Lecolley, J.F., Lefebvres, F., Louvel, M., Steckmeyer, J.C., Adloff, J.C., Bilwes, B., Bilwes, R., Glaser, M., Rudolf, G., Scheibling, F., Stuttge, L., Ferrero, J.L.: Nucl. Phys. A**488**, 255c (1988)
50. Ngo, Ch.: Nucl. Phys. A**348**, 140 (1980)
51. Royer, G., Mignen, J.: J. Phys. G**18**, 1781 (1992)
52. Ohlsen, G.G.: Nucl. Instr. Meth. **37**, 240 (1965)
53. Kun, S.Yu.: Phys. Lett. B**257**, 247 (1991)
54. Kun, S.Yu., Nöremberg, W.: Z. Phys. A**343**, 215 (1992)
55. Kun, S.Yu., Nöremberg, W., Papa, M.: Phys. Lett. B**298**, 273 (1993)
56. Rizzo, F., Cardella, G., De Rosa, A., Di Pietro, A., D'Onofrio, A., Fioretto, E., Inglima, G., Musumarra, A., Papa, M., Pappalardo, G., Romano, M., Romoli, M., Terrasi, F., Sandoli, M., Wang, G.S.: Z. Phys. A**349**, 169 (1994)
57. Vannucci, L., Abbondanno, U., Bettiolo, M., Bruno, M., Cindro, N., D'Agostino, M., Milazzo, P.M., Ricci, R.A., Ritz, T., Scheid, Vannini, G.: Z. Phys. A**355**, 41 (1996)
58. Kun, S.Yu., Abbondanno, U., Bruno, M., Cindro, N., D'Agostino, M., Milazzo, P.M., Ricci, R.A., Ritz, T., Robson, B.A., Scheid, W., Vavog, A.V., Vannini, G., Vannucci, L.: Z. Phys. A**359**, 145 (1997)